The Ninth Pacific Rim Conference On Stellar Astrophysics
ASP Conference Series, Vol. 451
S. B. Qian, K. C. Leung, L. Y. Zhu, and S. Kwow, eds.

The 100 Myr Star Formation History of NGC 5471

Rubén García-Benito,[1] Enrique Pérez,[2] Ángeles I. Díaz,[3]
Jesús Maíz Apellániz,[2] and Miguel Cerviño[2]

[1]*Kavli Institute of Astronomy and Astrophysics, Peking University, 100871, Beijing, China*

[2]*Instituto de Astrofísica de Andalucía, CSIC, Aptdo. Correos 3004, E-18080 Granada, Spain*

[3]*Departamento de Física Teórica (C-XI), Facultad de Ciencias, Universidad Autónoma de Madrid, Ctra. Colmenar Viejo km 15.600, E-28049 Madrid, Spain*

Abstract. Although NGC 5471 has been considered as a classical example of an instantaneous burst of star formation, we show that in addition to the most recent ionizing burst, star formation has been proceeding more or less continuously in NGC 5471 for at least 100 Myr. Using HST/WFPC2 F547M and F675W, ground based JHKs, and GALEX FUV and NUV images, we have conducted a photometric study of the star formation history of this giant HII region in M101. We perform an integrated analysis of the main emission knots and as a whole of NGC 5471, and a photometric study of the color-magnitude diagram (CMD) of the resolved stars. The integrated photometry for the whole region provides 2 different ages, revealing a complex star formation history, confirmed by the CMD resolved stellar photometry analysis. The spatial distribution of the stars shows that the star formation in NGC 5471 has proceeded along the whole region during, at least, the last 50-100 Myr. The current ionizing clusters are enclosed within a large bubble, which is likely to have been produced by the stars that formed ~20 Myr ago.

1. Introduction

Massive star forming regions are the source of much of what we know about the evolution of the universe. They are the cradle where most massive stars form and a major contributor to the chemical evolution of the universe. Because they are so energetic and luminous, those in the local universe, commonly known as Giant Extragalactic H II Regions (GEHRs), are intensively studied as tracers of the history of the star formation, of the chemical composition of the interstellar medium (including abundance gradients in galaxies), and as the best indicators of the conditions that lead to the formation of massive stars. GEHRs are characterized by sizes greater than 100 pc and by large Hα luminosities, implying that their giant ionized regions have large numbers of young massive stars, most of them born in Massive Young Clusters (MYCs), with an ionizing power equivalent to up to several thousand O5 V stars. Such a large stellar concentration provides an excellent laboratory to study the modes of massive star formation.

The energy deposited in the interstellar medium in the form of stellar winds, supernova explosions, and ultraviolet light produces complex stellar and gaseous spatial distributions which change rapidly during the few Myr following the onset of the first generation of massive stars. The massive young clusters that power the GEHRs are expected to form on a timescale shorter than 10 Myr, but increasingly more studies are revealing that all the stars in a given GEHR may not be coeval (Walborn et al. 2002).

M101 is a giant spiral galaxy located at a distance of 7.2 Mpc. This galaxy contains a large number of very luminous GEHRs, of which NGC 5471 is the outermost. The Hα morphology of NGC 5471 shows multiple cores with surrounding nebular filaments, extending over a diameter of $\sim$17″ ($\sim$600 pc). Ground-based photometry shows five bright knots, designated by Skillman (1985) as the A, B, C, D, and E components. The A component is as luminous as 30 Doradus and the B (which harbors a hypernova, Chen et al. 2002), C, and E components are comparable to NGC 604, the two prototypical spatially resolved mini-starbursts in the Local Group.

All these features make NGC 5471 an excellent candidate for the study of complex star formation, being close to the limit distance between the spatially well-resolved Local Group GEHRs and the more distant unresolved starbursts, thus providing an intermediate step in our understanding of very massive star-forming regions.

2. Results

2.1. Resolved stellar photometry

Hubble Space Telescope (HST) Wide Field Planetary Camera 2 (WFPC2) images of NGC 5471 were retrieved from the HST archive. The images were taken through two emission-line filters: F656N (Hα) and F673N ([S II]), and two continuum filters: F547M (Strömgren y) and F675W (WFPC2 R). The scale of the WF CCDs at NGC 5471, for which we assume a distance modulus of $(m - M) = 29.3$ (Stetson et al. 1998), is 3.5 pc pixel^{-1}.

The HST-pipeline WFPC2 images were subjected to the usual processing using the IRAF and STSDAS software packages. Given the luminosity of NGC 5471, its Hα and [SII] emission contributes significantly to the broad band (F675W) image. We used these narrow band images to eliminate the nebular contribution and obtain a new, emission line free, broad band image (F675W′).

Figure 1 (*left*) shows the Hα image. The five brightest components first noted by Skillman (1985) and designated as A, B, C, D and E, are distinctly observed in that figure. Previous works have associated X-ray sources with supernova remnants (SNRs) in M101. Chen et al. (2002) conclude that the energetic SNR in NGC 5471B was very likely produced by a hypernova.

The stellar photometric analysis was performed with the *HSTphot* package (Dolphin 2000). This package is specifically designed for use with HST WFPC2 images. The `hstphot` routine was run on the images in the F547M and F675W′ bands. This task performs stellar PSF photometry on multiple images from different filters, including alignment, aperture corrections, and geometric distortions.

We selected "good stars" from the `hstphot` output. To ensure that we only have point-like sources, we also used the "sharpness" parameter and a measure of the quality of the fit (χ^2) to reject false star detections in regions with structured nebulosity or artifacts.

We estimated the completeness in two different regimes of crowding: inside the core of the region[1] (dashed line in the left side of Figure 2) and in the rest of the image (solid line in left side of Figure 2).

To perform the statistical decontamination of the field stars, we followed the procedure described by Mighell et al. (1996) and Bellazzini et al. (1999).

2.2. Cluster photometry

JHK_s photometry was performed on 2000 April 29, using the 3.58m TNG (*Telescopio Nazionale Galileo*) at the Observatorio del Roque de los Muchachos in La Palma. The spatial scale was $0\farcs35$ pixel^{-1} and the field of view 90×90 arcsec^2.

We have derived the integrated magnitudes and colors in eleven different apertures covering the main components in the core of NGC 5471. The apertures were chosen and defined in the H-band image, maximizing the area in order to include the features of all images, since there were some small offsets in the position and intensity of the knots in the optical and infrared images respectively. Then, the same polygons were used for the J, K_s and HST images. The polygons defined are shown in the left side of Figure 1.

We have also measured the Hα flux for each polygon. To measure the integrated Hα flux of the whole region, we have decontaminated the F656N image from the broad band F675W contribution. A circular aperture centered in the region with radius 15 arcsec was defined. The flux measured inside this circular aperture is $(3.65 \pm 0.17) \times 10^{-12}$ erg cm^{-2} s^{-1}.

FUV and NUV images of M101 were retrieved from the Nearby Galaxies Survey (NGS). Due to the spatial scale (the GALEX point spread function translates to 160 pc at M101 distance), we only use the ultraviolet data to study the integrated photometry. We measured the FUV and NUV fluxes inside 15″ radii aperture centered in NGC 5471.

We have analyzed the integrated photometric measurements with the help of CHORIZOS, a code written in IDL by Maíz-Apellániz (2004). This code compares photometric data with model spectral energy distributions (SEDs), calculating the likelihood for the full parameter range specified, allowing for the identification of multiple solutions.

In the case of our study, we have used the STARBURST99 models (Leitherer et al. 1999). We fixed two parameters: the known metallicity of NGC 5471 and the type of dust ($R_V = 3.1$), leaving unconstrained the amount of extinction and the age. The metallicity of the region was assumed to be traced by the oxygen abundance. Detailed spectrophotometric studies give a mean value of 12+log(O/H) of 8.06 for three of the main knots (Kennicutt et al. 2003). Therefore we used the value $Z = 0.2Z_\odot$ in CHORIZOS.

[1]The core is defined as the inner ellipse in Figure 3.

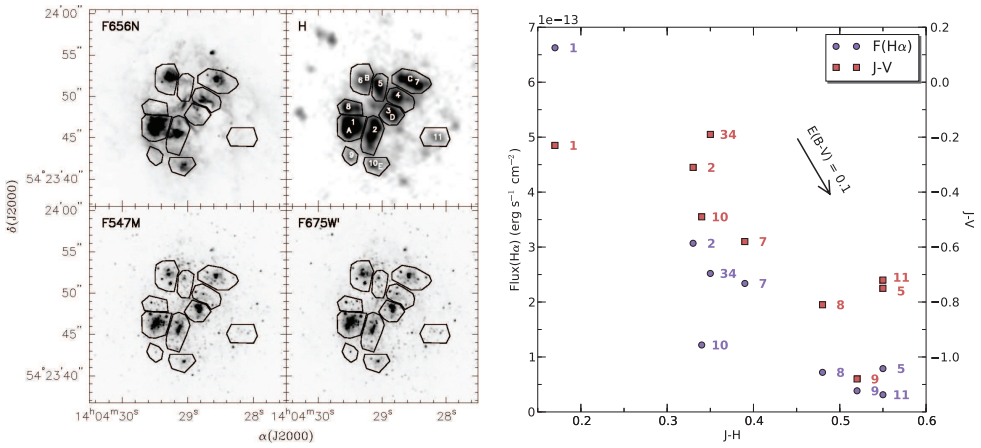

Figure 1. *Left.* Plot of the eleven polygons, limiting the different areas where the integrated magnitudes are computed. The numbers belong to our own definition while the A, B, C, D and E letters are the knots identified by Skillman (1985). The hypernova is located in knot 6. *Right.* Hα and J-V versus J-H plot for the clusters identified in the left side of the figure (V stands for the 547M filter). A clear correlation of decreasing Hα with redder colors points to an aging effect within the ongoing starburst phase. Reproduced by permission of the AAS.

3. Discussion

3.1. Cluster analysis

The integrated photometry analysis of the clusters may be affected by size of sample effects (Cerviño & Valls-Gabaud 2003) in some of the clusters (see García-Benito et al. 2011 for a detailed discussion). However, we present here the analysis to show, as a case of study, the possible interpretations.

CHORIZOS finds a most likely SSP with relatively high extinction and a young age 3 ± 2 Myr in the case we use only the optical-to-NIR photometry. If we include the FUV and NUV GALEX photometry then CHORIZOS finds two loci of maximum likelihood for a single SSP, one that corresponds to an age of 8 ± 2 Myr with moderate extinction and a second maximum at an age 60 ± 15 Myr and very low extinction. This result suggests that a significant fraction of the GALEX flux integrated within the 15 arcsec radius aperture from NGC 5471 is produced by a post-nebular stellar population of B stars (see also Waller et al. 1997).

The right side of Figure 1 shows a color-color-Hα plot of the individual clusters. The hypernova knot is not shown, and knots 3 and 4 have been combined into a single knot 34[2]. There is a clear correlation in the sense that redder knots have less Hα flux. The flux of Hα can decrease due to the aging of the burst or to different clusters having different masses, less massive bursts producing fewer ionizing photons. At any rate,

[2]The nature of knots 3+4 is not clear, it may be that both are part of the same cluster that has evolved sufficiently for the stellar winds to evacuate its center from ionized gas. Further higher spatial resolution IR and UV imaging is needed to establish more details.

more data in other clusters is needed to further explore this relationship with the infrared color.

Knot 1 is the brightest in Hα and the age estimations obtained by CHORIZOS give the youngest age, 3 ± 2 Myr, with the lowest extinction. For knots 2, 3, 4, 7, 8, 9, 10 CHORIZOS estimates an intermediate age, 5 ± 2 Myr, with an intermediate extinction, except may be knot 9 which has some indications for a somewhat higher extinction. Knots 5 and 11 have older age estimations, 9 ± 3 Myr. However, except for Knot 1, 2 and 34, the age estimations can also be explained by size-of-sample effects with under-luminous case (Villaverde et al. 2010). In these cases, age estimations, although apparently consistent, should not be considered as final, pending a more complete analysis with additional data sets.

3.1.1. Mass of the ionized gas

NGC 5471 is truly a cluster of superclusters with a luminosity $L_{\mathrm{H}\alpha}$~2.3×10^{40} erg s^{-1} (> 4×30 Doradus) and a total ionized gas mass $M_{\mathrm{HII}} \sim 5.5\times10^5$ $M_\odot$. This value and Díaz (1998) relation yield a mass of the ionizing stellar cluster in the range $0.6 - 1.1 \times 10^6$ $M_\odot$. Following the new calibration by Otí-Floranes & Mas-Hesse (2010), we obtained a Star Formation Strength of 2.3×10^6 $M_\odot$ for a burst of 5 Myr. If the region would be experiencing a continuous constant star formation, the Star Formation Rate (SFR) given by this calibration would be 0.1 $M_\odot$ yr^{-1}.

Thus, we find that the masses of ionized gas and of the stellar cluster in the current star formation event are both of the same order of magnitude, close to 10^6 $M_\odot$. This similarity may be understood in terms of a very high efficiency in star formation. Given that this is not the first event of star formation in NGC 5471 in the last 100 Myr, this high star formation efficiency takes an important meaning that implies that there has to be a large reservoir of gas to maintain this important star formation activity.

The H I distribution of M101 contains a large number of well-defined concentrations, with NGC 5471 being one of the brightest. The radio continuum thermal-H II emission source has the highest observed central emission measure of all the M101 complexes and an H I concentration of nearly 10^8 $M_\odot$ is closely coincident with this H II peak (Viallefond et al. 1981). The general distribution of the H I gas in M101 follows that of the diffuse FUV emission, with enhancements in the 21 cm line emission seen near FUV peaks. Smith et al. (2000)'s UIT FUV flux measurement is in good agreement with our GALEX measurement of 9.8×10^{-14} erg cm^{-2} s^{-1} Å^{-1}, being NGC 5471 the brightest FUV peak in M101. This is reflected in a decreased molecular content surrounding NGC 5471 which has been dissociated by the high star formation efficiency, the highest in M101 as calculated by Giannakopoulou-Creighton et al. (1999). In these respects NGC 5471 resembles a blue compact galaxy.

3.2. CMD

The photometry of the individual stars presented in the color-magnitude diagram, V-R vs. V, of Figure 2 (*left* panel) is a powerful tool to further understand the star formation history in NGC 5471. Our own set of isochrones, represented in the figure, have been divided into five age bins, (4-10, 10-25, 25-50, 50-75, 75-100) Myr, and drawn by their concave hull, shown with different colors. The right hand side of the figure shows the luminosity function, which peaks at $M_{547M} = 24$.

A glance at the CMD tell us that star formation has been proceeding continuously for the last 100 Myr. The diagram is populated by stars of $\sim 4 - 50$ $M_\odot$. We can readily

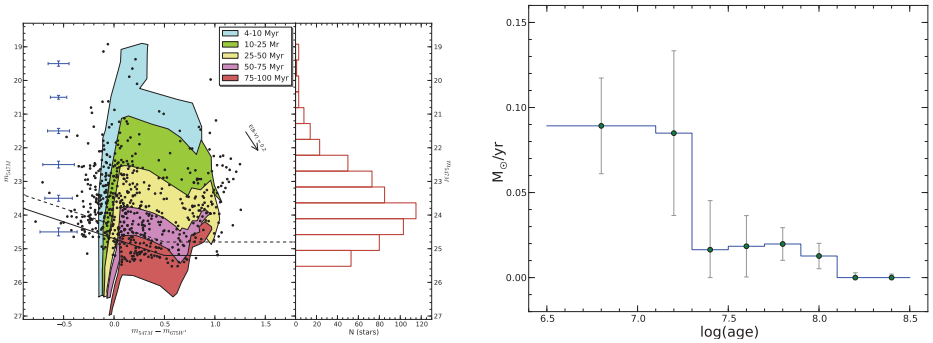

Figure 2. *Left.* Final CMD with isochrones divided into five age bins, drawn by their concave hull, and shown with different colors. Error bars correspond to an average error in each magnitude bin. The right hand side of the figure shows the luminosity function. The lines across the bottom show the completeness limit at the 50% level in the core (dashed line) and in the rest of the image (solid line). *Right.* STARFISH recovered Star Formation History of NGC 5471. Reproduced by permission of the AAS.

identify clear structures in the diagram. A well-defined main-sequence at V-R ∼ -0.1, which begins with the brightest star at 19 mag (∼ 4 Myr) and goes all the way down to 25 mag. Red stars span a range of 3 − 4 magnitudes in brightness, indicating that star formation has occurred during the last ∼ 15 − 70 Myr. There are some traces of the blue-plume at $M_V = -9$, indicating ongoing star formation. A strip of stars following a patch from [0.6,25] to [1.1,22.5] form the red giant branch.

3.2.1. Mass in stars and star formation history

We have used the code STARFISH (Harris & Zaritsky 2001) to find a best fit to the CMD by a linear combination of Hess diagrams at different ages. We have used our own set of isochrones. The best-fit SFH of NGC 5471 is shown in Figure 2 (*right* panel). The SFH derived seems to be consistent with a continuous one, but the errors only allow to take into consideration two episodes: a dominant young burst < 20 Myr, preceded by a longer event during the period 20-100 Myr. According to the SFR, the integrated mass in stars of the youngest event is comparable to the oldest one, with $\sim 10^6$ $M_\odot$.

Although this only gives an order of magnitude estimate, we can conclude that the integrated mass of stars formed in the past 20-100 Myr is of the order of magnitude of the current star formation event. If the star formation proceeds in an isolated gas cloud, we would expect that the rate at which stars form would decrease with time, as less gas is left available to form new stars. This is what is observed in many giant H II regions with two or more generations of star formation, where the latest event is less massive than the previous. In the case of NGC 5471 the results from the integrated photometry and from the CMD indicate that the current star forming event is as massive as those during the previous 20-100 Myr. We can understand this in the context of the large H I spiral arm in which the region is immersed. In this respect, Waller et al. (1997) conclude from a morphological study of M101 that NGC 5471 may be the result of tidal interactions of M101 with the nearby galaxies NGC 5477 and NGC 5474 in the time interval 100-1000 Myr ago.

3.2.2. Spatial distribution of the star formation history

Given the long duration of the star formation in NGC 5471 and its large size $\sim$ 1 kpc, it is natural to question the spatial location of the star formation through time along the extent of the region. We have selected four different areas in the CMD and proceeded to locate spatially the stars in these four boxes. Figure 3 displays the resulting distributions. The youngest and more massive stars (top-left panel) are clearly concentrated in the main star forming emission line knots, implying that massive stars are now forming mainly in clusters. The bottom-right panel displays the distribution of intermediate mass stars ($\sim 5 - 10$ $M_\odot$) older than about 50 Myr; these stars are distributed mainly towards the halo, with only a few in the core of the region. The top-right and bottom-left panels show the distribution of intermediate mass stars ($\sim 10 - 15$ $M_\odot$), both those which are in the main sequence and those which have already evolved out of it. The distributions of stars in these two CMD boxes are clearly concentrated fairly uniformly throughout the core of NGC 5471. Because the stars in these two intermediate boxes are of the same mass but they are found in a range of evolutionary stages, this implies that star formation has proceeded more or less uniformly in the core for the last $\sim 20 - 50$ Myr.

Star formation in the complex NGC 5471 has proceeded in a general spatio-temporal sequence from the periphery to the core. During the first epoch, $\sim 50 - 100$ Myr ago, the star formation occurred along the periphery and the core, then a second major event $\sim 10 - 20$ Myr ago was more or less uniformly distributed mainly in the core, and finally the current ionizing star forming event is mostly concentrated in the singular bright clusters located inside the core, where the gas reservoir is presumably higher. At the same time, we have seen from both the integrated photometry analysis and the CMD, that as the events proceeded concentrating from the periphery to the core clusters, the amount of mass of gas formed into stars seems to be of the same order of magnitude, but more concentrated in time, with higher star formation rate.

We note that the current event of ionizing clusters is apparently contained within a large bubble which defines the core of NGC 5471. This bubble, of projected size 400×550 pc (clearly defined geometrically and kinematically) is likely to have been produced by the stars that formed $\sim$ 20 Myr ago.

4. Conclusions

During the past few years evidence is accumulating that the scenario of formation of massive stars in several episodes is common in GEHRs. We have found a complex history of star formation for NGC 5471. Integrated photometry of the whole region, using data from GALEX (UV), HST/WFPC2 (optical), and TNG (NIR), yields one solution that corresponds to an age of 8 Myr and an older solution with an age around 60 Myr. From the photometric analysis of the eleven clusters defined on the IR H image a correlation emerges in the sense that the redder knots have a lower Hα flux, showing a clear aging trend. The ages range from 3 Myr for the youngest cluster to 10 Myr for the oldest one. The complex history of star formation of NGC 5471 revealed by the cluster analysis is confirmed by the resolved stellar analysis. The star formation history recovered through CMD reconstruction shows that star formation has been proceeding continuously for the last 100 Myr.

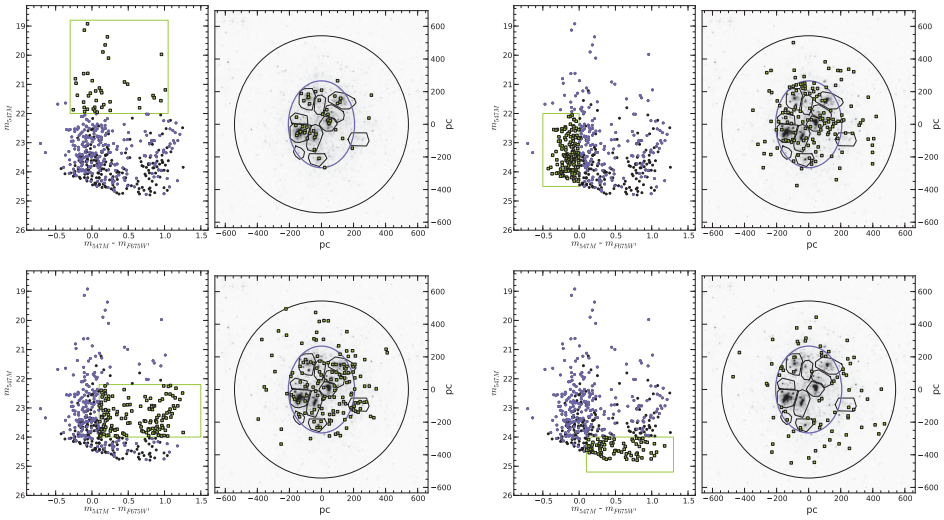

Figure 3. Spatial distribution of the star formation with time. The CMD contains only stars with magnitudes below the 50% completeness defined in the core region. The spatial distribution of the stars within four boxes selected in the CMD are shown in the right hand side images. The images are also drawn with a circle of 15 arcsec radius, indicating the area of the integrated photometry, an ellipse delineating the core region and the polygons selected for the cluster analysis. The square points represent the stars in the box selected in the CMD, the light color points indicate the stars located in the core of the region (inner ellipse), while the black points stand for the stars belonging to the halo. Reproduced by permission of the AAS.

Acknowledgments. RGB acknowledges support from the China National Postdoc Fund Grant No. 20100480144.

References

Bellazzini, M., Ferraro, F. R., & Buonanno, R. 1999, MNRAS, 307, 619
Cerviño, M., & Valls-Gabaud, D. 2003, MNRAS, 338, 481
Chen, C.-H. R., Chu, Y.-H., Gruendl, R., Lai, S.-P., & Wang, Q. D. 2002, AJ, 123, 2462
Díaz, Á. I. 1998, Ap&SS, 263, 143
Dolphin, A. E. 2000, PASP, 112, 1383
García-Benito, R., Pérez, E., Díaz, Á. I., Maíz Apellániz, J., & Cerviño, M. 2011, AJ, 141, 126
Giannakopoulou-Creighton, J., Fich, M., & Wilson, C. D. 1999, ApJ, 522, 238
Harris, J., & Zaritsky, D. 2001, ApJS, 136, 25
Kennicutt, R. C., Jr., Bresolin, F., & Garnett, D. R. 2003, ApJ, 591, 801
Leitherer, C., Schaerer, D., Goldader, J. D., Delgado, R. M. G., Robert, C., Kune, D. F., de Mello, D. F., Devost, D., & Heckman, T. M. 1999, ApJS, 123, 3
Maíz-Apellániz, J. 2004, PASP, 116, 859
Mighell, K. J., Rich, R. M., Shara, M., & Fall, S. M. 1996, AJ, 111, 2314
Otí-Floranes, H., & Mas-Hesse, J. M. 2010, A&A, 511, A61
Skillman, E. D. 1985, ApJ, 290, 449
Smith, D. A., Allen, R. J., Bohlin, R. C., Nicholson, N., & Stecher, T. P. 2000, ApJ, 538, 608
Stetson, P. B., Saha, A., Ferrarese, L., Rawson, D. M., Ford, H. C., Freedman, W. L., Gibson, B. K., Graham, J. A., Harding, P., Han, M., Hill, R. J., Hoessel, J. G., Huchra, J. P., Hughes, S. M. G., Illingworth, G. D., Kelson, D. D., Kennicutt, R. C., Jr., Madore, B. F.,

Mould, J. R., Phelps, R. L., Sakai, S., Silbermann, N. A., & Turner, A. 1998, ApJ, 508, 491
Viallefond, F., Allen, R. J., & Goss, W. M. 1981, A&A, 104, 127
Villaverde, M., Cerviño, M., & Luridiana, V. 2010, A&A, 522, A49
Walborn, N. R., Maíz-Apellániz, J., & Barbá, R. H. 2002, AJ, 124, 1601
Waller, W. H., Bohlin, R. C., Cornett, R. H., Fanelli, M. N., Freedman, W. L., Hill, J. K., Madore, B. F., Neff, S. G., Offenberg, J. D., O'Connell, R. W., Roberts, M. S., Smith, A. M., & Stecher, T. P. 1997, ApJ, 481, 169

Tour